ACS OMEGA

Open Access

http://pubs.acs.org/journal/acsodf

Article

NMR Analysis and Assignment of a Biosynthesis Gene Cluster for Trichokonins VI and VIII, Antiplasmodial Large Peptaibols Produced by a *Trichoderma* sp. Fungus

Ariane F. Bertonha, David E. Williams, Karen J. Nicacio, Marcelo R. de Amorim,* Sydney M. Schoellhorn,* Anna Caroline C. Aguiar, Talita Alvarenga Valdes, Giovana Rossi Mendes, Igor M. R. Moura, Lamonielli F. Michaliski, Matheus Gotha, Caue A. W. Zuccarino, Lara D. Sette, Antônio G. Ferreira, Raymond J. Andersen, Rafael Victorio Carvalho Guido,* and Roberto G. S. Berlinck*

Cite This: *ACS Omega* 2025, 10, 48293−48307

Read Online

ACCESS | Metrics & More | Article Recommendations | Supporting Information

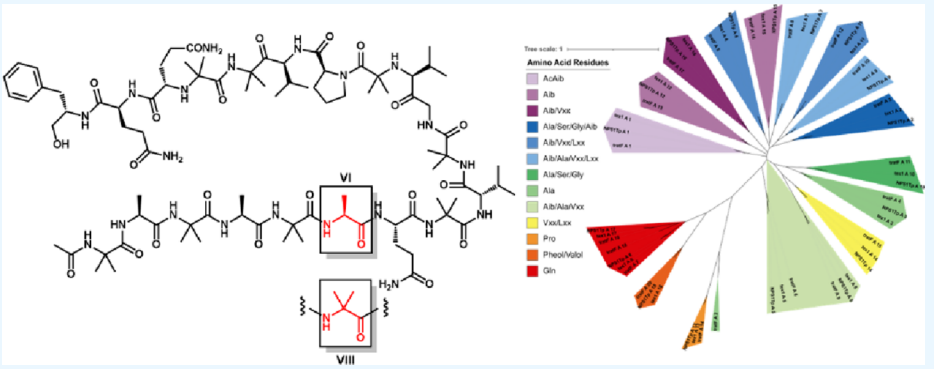

ABSTRACT: Peptaibols are modified linear peptides that typically include an acyl fragment connected at the *N*-terminal moiety, a reduced acid extremity and α-aminoisobutyric acid residues as common features, as well as other structural modifications. Peptaibols very often display potent biological activity, in particular, antimicrobial activity. Trichokonins VI (**1**) and VIII (**2**) are large peptaibols composed of 20 amino acids, which were previously only characterized by analysis of MS/MS data. We herein report the first full characterization of trichokonins VI (**1**) and VIII (**2**) by analysis of NMR data, along with an analysis by electronic circular dichroism and HRMS/MS data. Also, full genome sequencing and analysis of *Trichoderma* sp. L2-2 allowed us to identify a peptaibol biosynthesis gene cluster and the proposal for a biosynthetic assembly of trichokonins VI and VIII. Trichokonins VI and VIII also demonstrated antiplasmodial activity at the submicromolar range against *Plasmodium falciparum*.

INTRODUCTION

Polar organisms have been of increasing interest in biotechnology and natural products chemistry because of their unique biological traits, including the expression of enzymes and secondary metabolites, resulting from adaptations in an extreme environment.[1,2] Among the most investigated polar organisms, fungi from Antarctica stand up as producers of a number of unique enzymes and bioactive natural products.[1−4] New peptaibols of nine amino acid residues isolated from cultures of *Tridocherma asperellum*, new highly oxygenated polyketides produced in culture by *Penicillium crustosum* PRB-2, new epipolythiodioxopiperazine alkaloids produced by *Oidiodendron truncatum* GW3-13, the highly complex heptacyclic polyketide talaverrucin A from cultures of *Talaromyces* sp. HDN151403, and the very uncommon sesquiterpenoids bearing a very rare nitrobenzyl group isolated from cultures of *Aspergillus insulicola* HDN151418 represent some of the various outstanding metabolites produced by fungi from Antarctica.[4]

Trichoderma, and its anamorph *Hypocrea*, is a fungal genus found in a wide range of habitats. It is reported to include more than 200 individual described species.[5,6] Secondary metabolites produced by *Trichoderma* spp. have mainly been used commercially in biocontrol.[7−9] Additionally, *Trichoderma* spp. secondary metabolites present cytotoxic, antimicrobial,

Received: June 4, 2025
Revised: September 12, 2025
Accepted: September 25, 2025
Published: October 10, 2025

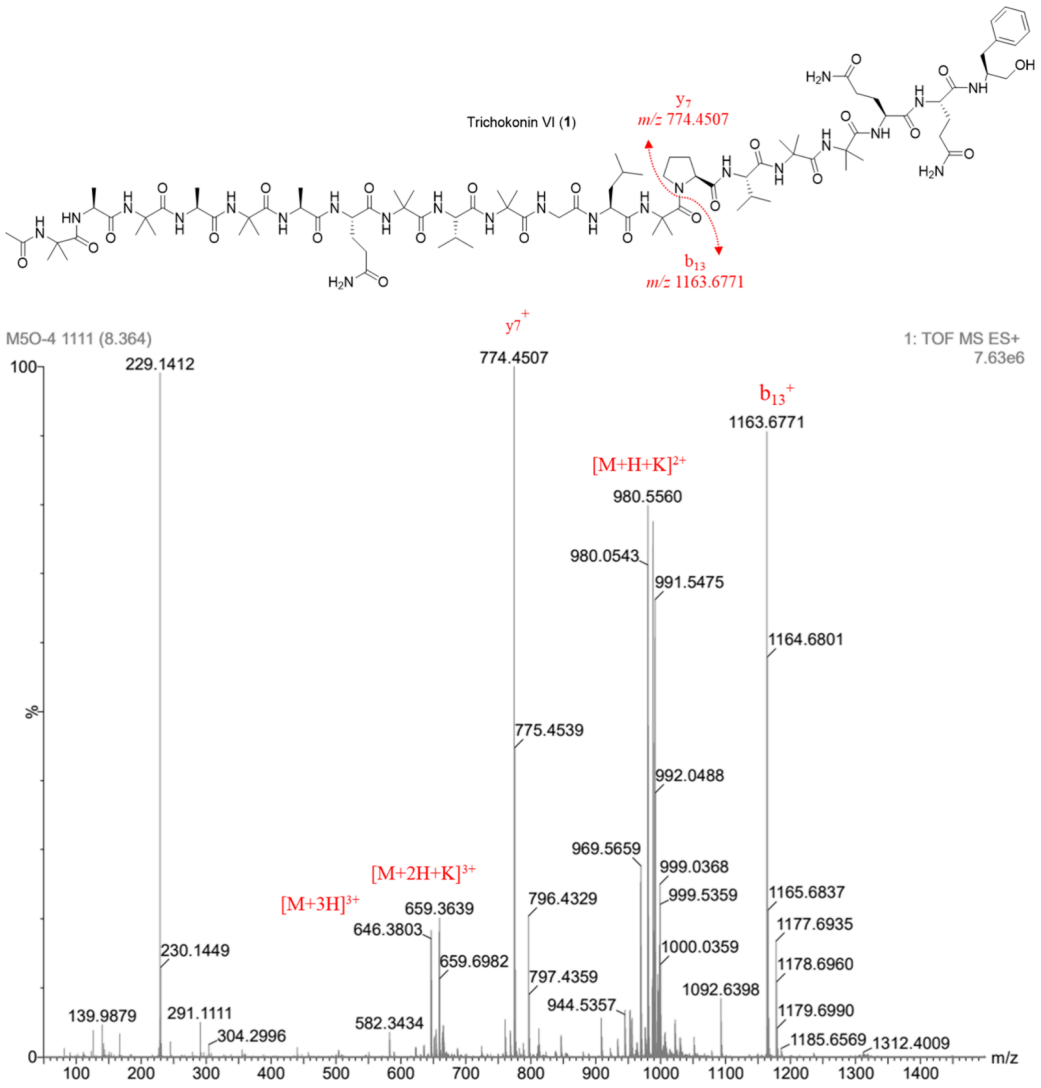

Figure 1. (+)-HRESIMS spectrum of trichokonin VI (**1**) indicating key fragments b_{13} and y_7.

and antioxidant activities, as well as metabolites enhancing plant growth.[10,11] Modified peptides known as peptaibols are commonly produced by *Trichoderma* species.[12−15] Peptaibols comprise a large peptide family, with over 1000 described peptidic entities, which can be linear or cyclic and are constructed from between 7 and 20 amino acid residues, many of which display cytotoxic and antibacterial activity.[16] Common features of peptaibols include the incorporation of α-aminoisobutyrate (Aib) residues, additional uncommon amino acids, an acylated *N*-terminus, and an amino alcohol of the reduced acid at the *C*-terminus.[16,17]

In our continuing search for bioactive secondary metabolites produced in culture by diverse fungi,[18−22] we have isolated trichokonins VI (**1**) and VIII (**2**), as well as additional peptaibols (**3**−**6**) from cultures of *Trichoderma* sp. L2-2, a strain obtained from a lichen sample collected at Admiralty Bay in Antarctica. Since no NMR data have been reported for trichokonins VI and VIII, we have performed complete NMR analyses to assign ^{1}H and ^{13}C, also the electronic circular dichroism (ECD) spectra, for both peptaibols, as well as their antiplasmodial activity. Additionally, we have also performed a bioinformatic analysis of *Trichoderma* sp. L2-2 genome and a putative biosynthetic gene cluster (BGC) related to the biosynthesis of trichokonins VI (**1**) and VIII (**2**) was assigned.

Previous investigations on trichokonins VI (**1**) and VIII (**2**) include isolation and identification by mass spectrometry analysis.[23] In that investigation, only trichokonin VII was identified by NMR analysis, but not trichokonins VI and VIII.[23] Trichokonin VI was reported with agonistic activity on L-type Ca^{2+} channels of cardiac membranes.[24] Optimal conditions for the production of trichokonins VI and VIII have been reported.[25] The cytotoxicity mechanism of trichokonin VI on hepatocellular carcinoma (HCC) cells has been investigated. Trichokonin VI inhibits the growth of HCC cells in a dose-dependent manner. Apoptosis and autophagy are the likely mechanisms involved in trichokonin VI cytotoxic activity.[26] Trichokonin VI also induces apoptosis in cells of the plant fungal pathogen *Fusarium oxysporum*[27] and presents a growth-inhibitory effect on *Arabidopsis* primary roots by inhibiting cell division and elongation processes.[28] It was also verified that trichokonin VI increased the auxin content and promoted disturbance in auxin signaling gradients within root tips.[28] The same peptaibol promotes the growth and induces a systemic resistance against the gray mold disease caused by the fungus *Botrytis cinerea* in *Phalaenopsis* orchids.[29] Also, both

https://doi.org/10.1021/acsomega.5c05271
ACS Omega 2025, 10, 48293−48307

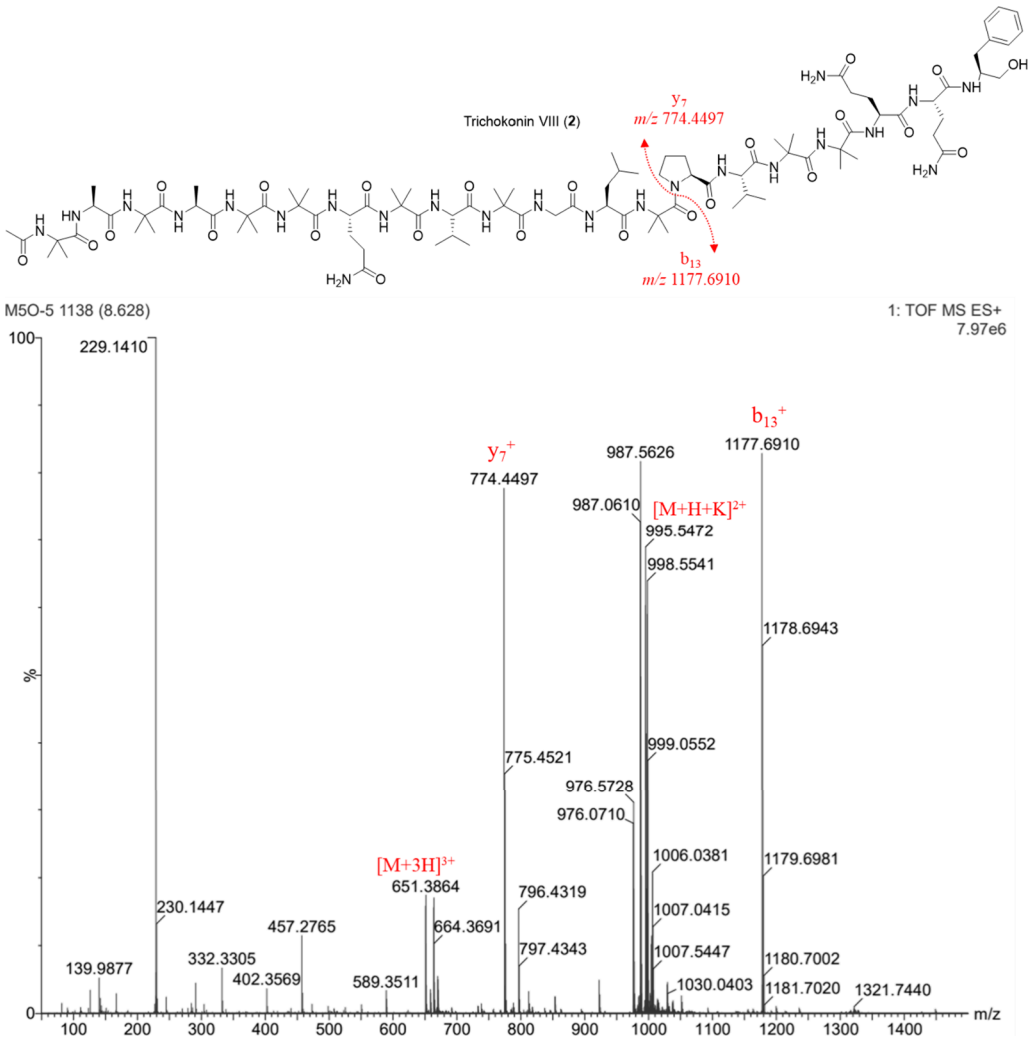

Figure 2. (+)-HRESIMS spectrum of trichokonin VIII (**2**) indicating key fragments b_{13} and y_7.

peptaibols **1** and **2** displayed genotoxic activity on ovary CHO-K1 cancer cells.[30] In the case of trichokonin VIII (**2**), its ^{1}H and ^{13}C NMR spectra were recently reported, but the data were not assigned, although its extensive MS/MS analysis was presented.[31]

RESULTS AND DISCUSSION

Isolation and Complete Characterization of Trichokonins VI and VIII. The EtOAc-soluble extract of cultures of *Trichoderma* sp. L2-2 was fractionated on a silica-gel-bonded cyanopropyl column to give six fractions. Fraction AT1M5 indicated compounds with a molecular weight higher than 500 Da by HPLC-MS analyses. This fraction was subjected to a separation and purification procedure (see the Experimental Section) that led to the isolation of trichokonin VI (**1**) and trichokonin VIII (**2**). The peptaibols trichogin A IV (**3**),[32,33] hypocrin NPDG F (**4**),[34] hypocrin NPDG H (**5**),[35] and trikoningin KB I (**6**)[35,36] were also isolated and identified by analysis of spectroscopic and spectrometric data and by comparison with literature data.

Trichokonins VI and VIII were isolated as white, amorphous powders. Their HRMS-(+) spectra exhibited pseudomolecular ions at *m/z* 774.4507 for **1** and *m/z* 774.4497 for **2** (Figures 1 and 2). This ion was likewise observed in the mass spectra of various peptaibol compounds produced by members of the *Longibrachiatum* clade of the filamentous fungus genus *Trichoderma*, such as alamethicin F50, trilongins BI and BIII, some trichoaureocins, suzukacillins, longibrachins, trichokonins, paracelsins, and others.[37,38] The mass spectra of 20-residue peptaibols often display characteristic features, including the fragmentation of the secondary amide bond between Aib[13]-Pro[14].[39] Proline residues are often found in long-chain peptaibols (7% of the composition), usually in the middle of the amino acid chain.[17] MS cleavage at the Pro residue leads to the formation of "acylium ion"-type fragments, which are usually considered as diagnostic peaks for the characterization of long-chain peptaibols. The MS values at *m/z* 774.4507 for **1** and *m/z* 774.4497 for **2** correspond to the C-terminal sequence Pro-Val-Aib-Aib-Gln-Gln-Pheol. To determine the complete sequence of the two complementary charged fragments, b_{13} and y_7, fragmentation of the complementary pseudomolecular ions of the isolated peptides was performed. Fragmentation of the pseudomolecular ions at *m/z* 1163.6771 for **1** (Figure S8) indicated the AA sequence Ac-Aib-Ala-Aib-Ala-Aib-Ala-Gln-Aib-Val-Aib-Gly-Leu-Aib, known as trichokonin VI. MS fragmentation of the pseudomolecular ion at *m/z* 1177.6910 of compound **2** indicated the sequence Ac-Aib-Ala-Aib-Ala-Aib-Aib-Gln-Aib-Val-Aib-Gly-Leu-Aib, corresponding to trichokonin VIII (Figure S21).

https://doi.org/10.1021/acsomega.5c05271
ACS Omega 2025, 10, 48293−48307

Table 1. ^{1}H (600 MHz) and ^{13}C (150 MHz) NMR Data for Trichokonin VI (1) (DMSO-d_6)

	position	δ_C	δ_H (J in Hz)		position	δ_C	δ_H (J in Hz)		position	δ_C	δ_H (J in Hz)		position	δ_C	δ_H (J in Hz)		position	δ_C	δ_H (J in Hz)
Ac	CH_3	23.1	1.92 s	Gln[7]	NH		7.95	Leu[12]	NH		7.72 d (7.7)	Aib[16]	NH		7.59	Gln[19]	NH		7.50, d (7.7)
	C=O	170.6			α CH	56.3	3.77		α CH	51.5	4.29		α C	55.4			α CH	53.5	3.96
Aib[1]	NH		8.62		β_1 CH_2	25.8	1.98		β_1 CH_2	39.8	1.41		β_1 CH_3	22.6	1.30−1.48		β_1 CH_2	26.9	1.78
	α C	55.4			β_2 CH_2	25.8	2.13		β_2 CH_2	39.8	1.81		β_2 CH_3	26.5	1.49		β_2 CH_2	26.9	1.88
	β_1 CH_3	26.5	1.43		γ_1 CH_2	31.0	2.15		γ CH	24.0	1.77		C=O	175.7			δ_1 CH_2	31.7	1.98
	β_2 CH_3	25.8	1.43		γ_2 CH_2	31.0	2.29		δ_1 CH_3	20.9	0.82 d (6.5)	Aib[17]	NH		7.86		δ_2 CH_2	31.7	2.28
	C=O	176.1			C(O) NH_2	173.2	6.73 s, 7.15 s		δ_2 CH_3	22.9	0.86 d (6.5)		α C	55.8			C(O) NH_2	173.7	6.73, s; 7.15, s
Ala[2]	NH		8.60		C=O	173.8			C=O	172.9			β_1 CH_3	26.3	1.39		C=O	170.9	
	α CH	51.8	3.95	Aib[8]	NH		7.87	Aib[13]	NH		8.17, s		β_2 CH_3	22.9	1.47	Pheol[20]	NH		6.95, d (8.8)
	β_1 CH_3	16.3	1.32 d (7.2)		α C	55.9			α C	56.1			C=O	175.5			α CH	52.3	3.89
	C=O	174.9			β_1 CH_3	22.9	1.36		β_1 CH_3	22.6	1.30−1.48	Gln[18]	NH		7.61		β_1 CH_2	36.7	2.54, dd (9.0, 13.6)
Aib[3]	NH		7.96		β_2 CH_3	26.5	1.42		β_2 CH_3	23.7	1.35		α CH	54.7	3.85		β_2 CH_2	36.7	2.91, dd (4.7, 13.6)
	α C	55.4			C=O	175.4			C=O	173.5			β_1 CH_2	26.5	1.97		C-1	139.1	
	β_1 CH_3	25.8	1.30−1.48	Val[9]	NH		7.30 br d (5.4)	Pro[14]	α_1 CH_2	48.5	3.55		β_2 CH_2	26.5	1.97		C-2, C-6	129.2	7.22
	β_2 CH_3	22.9	1.30−1.48		α CH	62.7	3.62 dd (6.5, 8.7)		α_2 CH_2	48.5	3.73		δ_1 CH_2	31.6	2.10		C-3, C-5	127.9	7.19
	C=O	175.7			β CH	28.7	2.20		β CH_2	25.5	1.87		δ_2 CH_2	31.6	2.30		C-4	125.8	7.13 dt (1.4, 7.2)
Ala[4]	NH		7.88		γ_1 CH_3	19.1	0.88 d (6.5)		γ_1 CH_2	28.7	1.68		C(O) NH_2	173.3	6.62, s; 7.07, s		γ_1 CH_2	63.0	3.32
	α CH	51.8	3.90		γ_2 CH_3	19.6	1.02 d (6.5)		γ_2 CH_2	28.7	2.22		C=O	172.0			γ_2 CH_2	63.0	3.34
	β_1 CH_3	16.5	1.41		C=O	173.0			δ CH	62.6	4.28						OH		4.62[a]
	C=O	175.1		Aib[10]	NH		8.03 s		C=O	173.4									
Aib[5]	NH		7.59 s		α C	55.8		Val[15]	NH		7.59								
	α C	56.0			β_1 CH_3	25.8	1.43		α CH	61.1	3.77								
	β_1 CH_3	25.7	1.41		β_2 CH_3	22.6	1.30−1.48		β CH	28.6	2.25								
	β_2 CH_3	23.0	1.48		C=O	175.9			γ_1 CH_3	19.0	0.89								
	C=O	172.6		Gly[11]	NH		8.13 t (5.7)		γ_2 CH_3	19.1	0.95								
Ala[6]	NH		7.94		α_1 CH_2	43.8	3.51		C=O	175.7									
	α CH	52.2	3.89		α_2 CH_2	43.8	3.75												
	β_1 CH_3	16.2	1.35		C=O	169.6													
	C=O	176.1																	

[a]Possible OH chemical shift.

https://doi.org/10.1021/acsomega.5c05271
ACS Omega 2025, 10, 48293−48307

Table 2. ^{1}H (600 MHz) and ^{13}C (150 MHz) NMR Data for Trichokonin VIII (2) (DMSO-d_6)

	position	δ_C	δ_H (J in Hz)		position	δ_C	δ_H (J in Hz)		position	δ_C	δ_H (J in Hz)		position	δ_C	δ_H (J in Hz)		position	δ_C	δ_H (J in Hz)
Ac	CH_3	23.2	1.86 s	Gln[7]	NH		7.68 d (4.1)	Leu[12]	NH		7.62 d (7.9)	Aib[16]	NH		7.52 s	Gln[19]	NH		7.43 d (7.6)
	C=O	170.6			α CH	56.4	3.68		α CH	51.5	4.23		α C	55.9			α CH	53.5	3.89
Aib[1]	NH		8.55 s		β_1 CH_2	25.9	1.89		β_1 CH_2	39.8	1.41		β_1 CH_3	26.5	1.40		β_1 CH_2	26.9	1.69
	α C	55.4			β_2 CH_2	25.9	1.98		β_2 CH_2	39.8	1.74		β_2 CH_3	22.1	1.30		β_2 CH_2	26.9	1.79
	β_1 CH_3	26.5	1.29		γ_1 CH_2	31.2	2.11		γ CH	24.1	1.71		C=O	175.0			δ_1 CH_2	31.6	1.91
	β_2 CH_3	26.0	1.32		γ_2 CH_2	31.2	2.26		δ_1 CH_3	20.9	0.76 d (6.1)	Aib[17]	NH		7.52 s		δ_2 CH_2	31.6	2.03
	C=O	176.1			C(O)NH_2	173.3	6.68 s, 7.00 s		δ_2 CH_3	22.9	0.81 d (6.1)		α C	56.0			C(O)NH_2	173.3	6.56 s, 7.08 s
Ala[2]	NH		8.51 d (5.3)		C=O	173.8			C=O	172.9			β_1 CH_3	26.5	1.42		C=O	171.0	
	α CH	51.8	3.88	Aib[8]	NH		7.86 s	Aib[13]	NH		8.09 s		β_2 CH_3	25.7	1.35	Pheol[20]	NH		6.89 d (9.0)
	β_1 CH_3	16.4	1.27 d (7.0)		α C	55.6			α C	56.1			C=O	175.7			α CH	52.3	3.84
	C=O	174.8			β_1 CH_3	26.6	1.29–1.42		β_1 CH_3	23.0	1.29–1.40	Gln[18]	NH		7.55 d (5.0)		β_1 CH_2	36.7	2.48 dd (8.4, 13.5)
Aib[3]	NH		7.85 s		β_2 CH_3	22.9	1.29–1.42		β_2 CH_3	23.7	1.29–1.40		α CH	54.7	3.79		β_2 CH_2	36.7	2.84 dd (4.5, 13.5)
	α C	55.6			C=O	175.6			C=O	173.4			β_1 CH_2	26.5	1.87		C-1	139.1	
	β_1 CH_3	25.9	1.37	Val[9]	NH		7.19 d (6.9)	Pro[14]	α_1 CH_2	48.5	3.47		β_2 CH_2	26.5	1.92		C-2, C-6	129.2	7.22
	β_2 CH_3	22.9	1.29–1.40		α CH	62.2	3.62 t (7.5)		α_2 CH_2	48.5	3.66		δ_1 CH_2	31.7	2.15		C-3, C-5	127.9	7.19
	C=O	175.7			β CH	28.6	2.18		β CH_2	25.5	1.80		δ_2 CH_2	31.7	2.26		C-4	125.8	7.13 dt (1.4, 7.2)
Ala[4]	NH		7.78 d (4.5)		γ_1 CH_3	19.1	0.90 d (6.5)		γ_1 CH_2	28.6	1.61		C(O)NH_2	173.7	6.71 s, 7.11 s		γ_1 CH_2	63.0	3.25
	α CH	51.9	3.84		γ_2 CH_3	19.4	0.92 d (6.5)		γ_2 CH_2	28.6	2.16		C=O	172.0			γ_2 CH_2	63.0	3.29
	β_1 CH_3	16.3	1.27 d (7.0)		C=O	173.0			δ CH	62.5	4.29						OH		4.55 br s
	C=O	174.9		Aib[10]	NH		7.84 s		C=O	173.4									
Aib[5]	NH		7.81 s		α C	55.6		Val[15]	NH		7.52								
	α C	55.6			β_1 CH_3	25.9	1.29–1.42		α CH	61.1	3.71								
	β_1 CH_3	26.0	1.41		β_2 CH_3	22.7	1.29–1.42		β CH	28.6	1.71								
	β_2 CH_3	22.6	1.48		C=O	175.9			γ_1 CH_3	19.0	0.81 d (6.5)								
	C=O	172.6		Gly[11]	NH		8.15 t (5.9)		γ_2 CH_3	19.0	0.83 d (6.5)								
Aib[6]	NH		7.83 s		α_1 CH_2	43.8	3.44		C=O	175.4									
	α C	55.6			α_2 CH_2	43.8	3.69												
	β_1 CH_3	26.9	1.40		C=O	169.6													
	β_2 CH_3	26.0	1.31																
	C=O	176.6																	

https://doi.org/10.1021/acsomega.5c05271
ACS Omega 2025, 10, 48293−48307

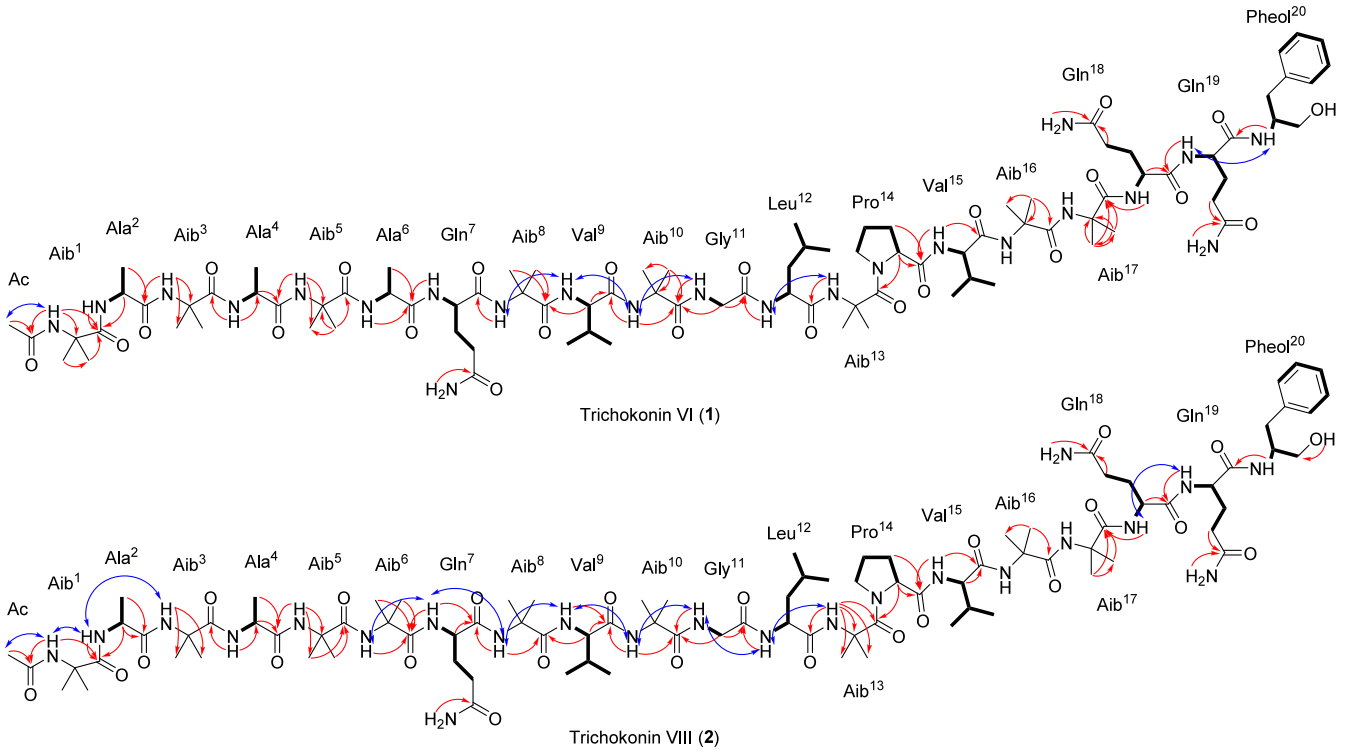

Figure 3. Key HMBC (red arrows), HSQC-TOCSY and COSY correlations (bold bonds), and NOESY (blue arrows) interactions for **1** and **2**.

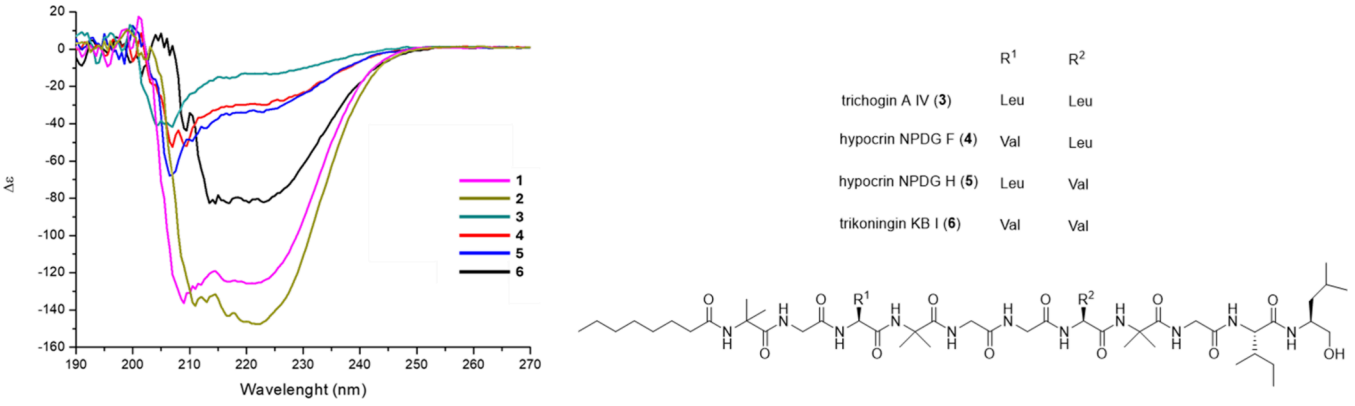

Figure 4. (Left) Circular dichroism spectra for peptaibols **1**−**6** in MeOH (c = 0.5 mg mL^{-1}). Chemical structures of lipopeptaibols **3**−**6**.

The specific rotation measured for trichokonin VI (**1**) was $[\alpha]_D^{21}$ = −9.0 (c 0.02, MeOH), while the literature-reported value was $[\alpha]_D^{20}$ = −10.0 (c 0.2, MeOH).[40] As for trichokonin VIII (**2**), the measured specific rotation was $[\alpha]_D^{21}$ = −23.0 (c 0.02, MeOH), with no data found in the literature. Marfey's analysis of both peptaibols **1** and **2** indicated the absolute stereochemistry of all proteinogenic amino acids as L (S) (see the Supporting Information).

Analysis of the NMR data of trichokonins VI and VIII enabled us to completely assign the ^{1}H and ^{13}C signals of both peptides for the first time (Tables 1 and 2).

The ^{1}H NMR spectra of trichokonins VI (**1**) and VIII (**2**) displayed 25 amide proton signals (from δ_H 6.56 to 8.62), overlapping α-proton signals (from δ_H 3.43 to 4.29), acetyl protons (δ_H 1.93 for **1** and δ_H 1.86 for **2**), overlapping γ-proton signals (δ_H 1.41 to 1.90), overlapping α-aminoisobutyric acid and alanine methyl groups (from δ_H 1.26 to 1.49) as well as leucine and valine methyl groups from δ_H 0.76 to 1.01 (Tables 1 and 2). Analysis of ^{13}C NMR data revealed 23 amide carbonyl signals (from δ_C 169.6 to 176.6), four sp^2 carbons (from δ_C 125.8 to 139.1) and one γ-carbon (δ_C 63.0) belonging to the pheol^{20} residue, 20 tertiary or quaternary α-carbons (from δ_C 48.5 to 62.7), and other methylene and methyl carbons from δ_C 16.2 to 39.8 (Tables 1 and 2). Based on the HSQC, HMBC, HSQC-TOCSY, COSY, and ROESY experiments, the amino acid residues Ala^2, Ala^4, Ala^6 (only for **2**), Gln^7, Val^9, Gly^{11}, Leu^{12}, Pro^{14}, Val^{15}, Gln^{18}, Gln^{19}, and Pheol^{20} could be confidently assigned (Figure 3). The Ac-Aib^1 and the other Aib amino acid residues in the trichokonins VI and VIII were defined by analyses of HSQC and HBMC correlations, the latter helping to position the Aib residues by observing cross peaks from adjacent amino acids (Figure 3), along with ROESY correlations.

Peptaibols exhibit circular dichroism spectra characteristic of helical peptide structures, with negative Cotton effects observed between 205 and 209 and 221−226 nm, and positive

https://doi.org/10.1021/acsomega.5c05271
ACS Omega 2025, 10, 48293−48307

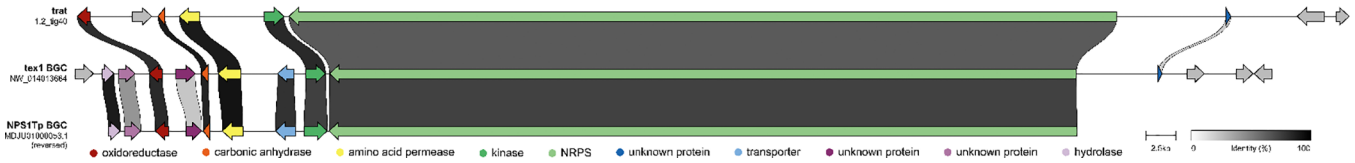

Figure 5. Clinker comparison of the peptaibol BGC identified in *Trichoderma* sp. L2-2 and other peptaibol BGCs.[45,46,48]

Table 3. Annotation and Comparison of the *trat* Biosynthetic Gene Cluster

gene	protein name	putative function	homologue	identity (%)	query cover (%)	*E*-value	score
tratA	TratA	aldo/keto reductase	T069G_08187	86.14	100	0	624
tratT	TratT	MFS general substrate transporter	K444DRAFT_652276	47.95	97	1e-162	485
tratB	TratB	carbonic anhydrase	T069G_08189	86.98	99	3e-106	311
tratC	TratC	amino acid permease	T069G_08190	93.77	100	0	999
tratD	TratD	Ppx/GppA phosphatase	T069G_08191	86.62	100	0	1016
tratS	TratS	NRPS	Tex1	76.96	100	0	26,904
tratE	TratE	unknown					
tratF	TratF	cytochrome P450	TGAM01_v204900	88.58	100	0	1077
tratG	TratG	*Ubia Prenyltransferase*	HER10_EVM0011648	47.43	98	1e-98	305

Cotton effect between 192 and 198 nm.[41] Since peptaibol skeletons are very well structured by the formation of hydrogen bonds and by the presence of the Aib residues, peptaibol CD spectra generally show minimal dependence on solvent variations. For peptaibols **1**, **2**, and **6** (Figure 4), we verified that the CD spectra exhibit a minimum at 209−211 nm, an extended minimum at 220−222 nm referring to the n-p* type transition, and a positive maximum absorption at approximately 194 nm typically observed for a α-helical peptidic conformation.[41] The CD spectra of peptaibols **1** and **2** are comparable in shape, position, and magnitude of the Cotton effect. CD spectra of compounds **3**−**5** (Figure 4) exhibit two minimum Cotton effect bands around 205−209 nm referring to p-p*-type transitions, accompanied by a discrete minimum between 220 nm referring to the n-p* type transition. A positive maximum near 194 nm, characteristic of a α-helix conformation,[41] has also been observed, confirming that peptaibols **1**−**6** all have *a*-helix structures in solution.

Genome Mining and Biosynthesis Gene Cluster Assignment of Trichokonins VI and VIII. The whole genome sequencing and processing of *Trichoderma* sp. L2-2 was performed by using Illumina and Nanopore technologies. The final assembly has 37,716,117 base pairs (bp) in 45 contigs, with a CG content of 47.6%. Analysis using fungiSMASH[42] identified 36 biosynthetic gene clusters (BGCs) (Figure 5), including 8 related to NRPS biosynthesis, 4 for NRPS-like, 10 for T1PKS, 6 for terpenes, 1 for fungal RiPP-like, 1 for isocyanide-nrp, and 6 hybrid BGCs. The hybrid BGCs included 3 NRPSs/T1PKSs, 1 NRPS-like/T1PKS, 1 NRPS-like/fungal RiPP-like, and 1 fungal RiPP-like/terpene. Interestingly, from the 3 NRPSs/T1PKSs BGCs, only 1 BGC located on scaffold 1 and contig 2 (1.2) contained a hybrid polyketide nonribosomal peptide synthase (PKS-NRPS) gene with the domain organization of 21-module PKS-NRPS (Figures S41−S43), potentially corresponding to trichokonins VI (**1**) and VIII (**2**) biosynthesis. This BGC was named *trat* (GenBank accession no. PX023957).

The *trat* BGC was refined using Augustus,[43] and NCBI's BLASTp tool[44] was used to evaluate coding sequences for homology to characterized proteins, which resulted in putative function annotations (Table 3). The *trat* cluster revealed nine open reading frames that encode the PKS-NRPS TratS, two oxidoreductases (TratA and TratF), three transporter proteins (TratT, TratB and TratC), a phosphatase (TratD), a prenyltransferase (TratG), and one unknown protein. A closer inspection of TratS (69.6 kb PKS-NRPS) showed an acyl transferase (AT) domain in the loading module for the incorporation of the acetyl group in the *N*-terminus and a reductase domain in the last module for converting *C*-terminal L-Phe to L-phenol, essential for 20-res peptaibol trichokonins VI and VIII synthetase. Additionally, the homology search of TratS showed 76% of identity with Tex1 peptaibol NRPS from *Trichoderma virens* Gv29-8 related to the production of 18mer peptaibols.[45,46]

Detailed comparative gene cluster analysis of the putative peptaibol BGC (*trat*) was performed against known peptaibols BGCs using Clinker[47] confirming high homology between the clusters (Figure 5). The NRPS gene Tex1 from *Trichoderma virens*[45,46] and $NPS1_{tp}$ from *Trichoderma pleuroti*[48] related to the production of peptaibols showed synteny with NRPS TratF with high identity.

The biosynthesis of trichokonins VI and VIII therefore is herein hypothesized to start from the *trat* BGC (Scheme 1), showing the domain organization of the 21-module PKS-NRPS TratS. The coisolation of trichokonins VI and VIII indicates that module 6 of the NRPS is capable to get two different amino acids, the Aib for trichokonin VI and the Ala for trichokonin VIII.

Phylogenetic analyses of the A and C domains of TratS, Tex1, and $NPS1_{Tp}$ (Figures 6 and 7) revealed greater similarity in module origin than in substrate specificity. There are some notable clades of more structurally distinct amino acid residues such as proline and glutamine, but the remaining residues demonstrate significant overlap between clades. The A and C domains from module 6 (TratS A6 and TratS C6), which have relaxed substrate specificity, formed clades with A and C domains related to the Ala, Alib, and Vxx amino acid residues. In a comparison of the phylogenetic distribution between the A and C domains, a difference can be noted in the designation of domains TratS A2 and TratS A3.

Antiplasmodial and Cytotoxic Activity of Trichokonins VI and VIII. Trichokonins VI (**1**) and VIII (**2**) were tested *in vitro* against *Plasmodium falciparum* (*P. falciparum*) (3D7 strain, chloroquine-sensitive) and human hepatocellular

https://doi.org/10.1021/acsomega.5c05271
ACS Omega 2025, 10, 48293−48307

Scheme 1. Proposed Biosynthesis for Trichokonins VI and VIII

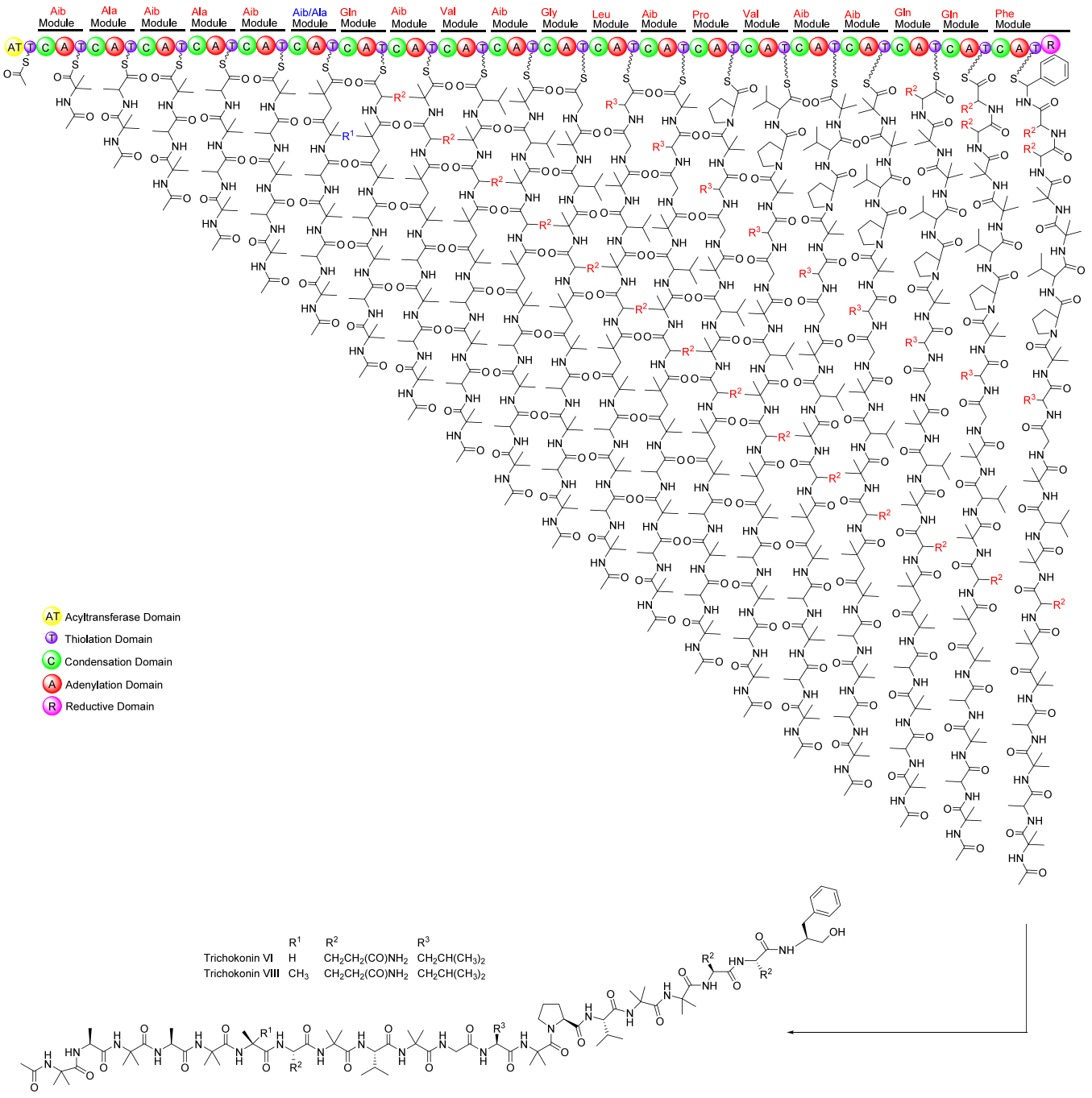

carcinoma cells (HepG2) to assess their antiplasmodial and cytotoxic activities (Table 4).

Trichokonins analogues demonstrated inhibitory activity against *P. falciparum* at low micromolar concentrations (IC_{50}s = 0.9−5.7 μM). Notably, trichokonins VI (**1**) and VIII (**2**) were the most potent derivatives, showing IC_{50}s values of 1.0 and 0.9 μM, respectively (Table 4). These results are consistent with previously reported antiplasmodial activity of peptaibols.[34,49] Furthermore, trichokonins exhibited moderate cytotoxic activity against HepG2 cells (CC_{50}^{HepG2} > 12 μM) (Table 4). Particularly, trichokonins VI (**1**) and VIII (**2**) demonstrated CC_{50}s values of 28 and 15 μM, respectively, resulting in selectivity indexes (SI) of 28 and 16, respectively. Compounds with SI values higher than 10 are considered promising for further investigations of new candidates for antimalarial drugs.[50]

Large-size peptaibols, with 18−20 amino acid residues, are numerous, with tens of such peptides been reported in the literature.[51−53] However, as far as we know, our results are the first to report antiplasmodial activity for large-size peptaibols with 20 amino acid residues. Since this activity is similar to previously reported peptaibols,[34,49] and that the structures of these compounds are similar, we suppose that the mechanism of action of our compounds is similar as well,[49] but this hypothesis remain to be confirmed. Although many of such large peptides have been isolated and identified, to the best of our knowledge, there are no reports on the structures of 20 amino acid residue peptaibols completely assigned by NMR,

https://doi.org/10.1021/acsomega.5c05271
ACS Omega 2025, 10, 48293−48307

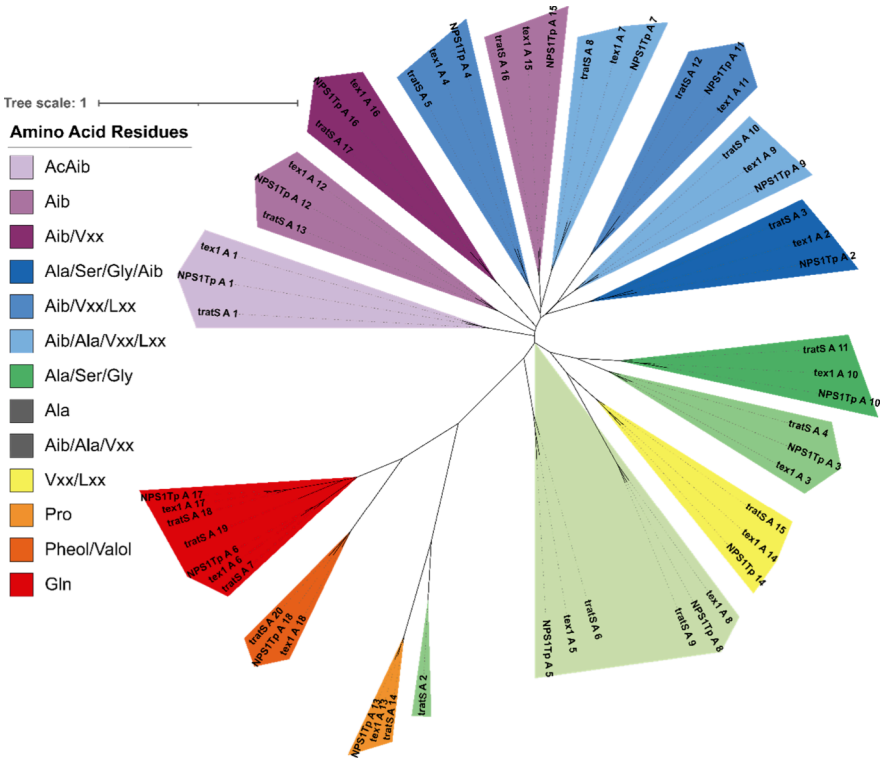

Figure 6. Phylogenetic analysis of the A domains from TratS, Tex1, and NPS1$_{Tp}$, color coded by substrate specificity. Vxx refers to valine or isovaline, and Lxx refers to leucine or isoleucine.

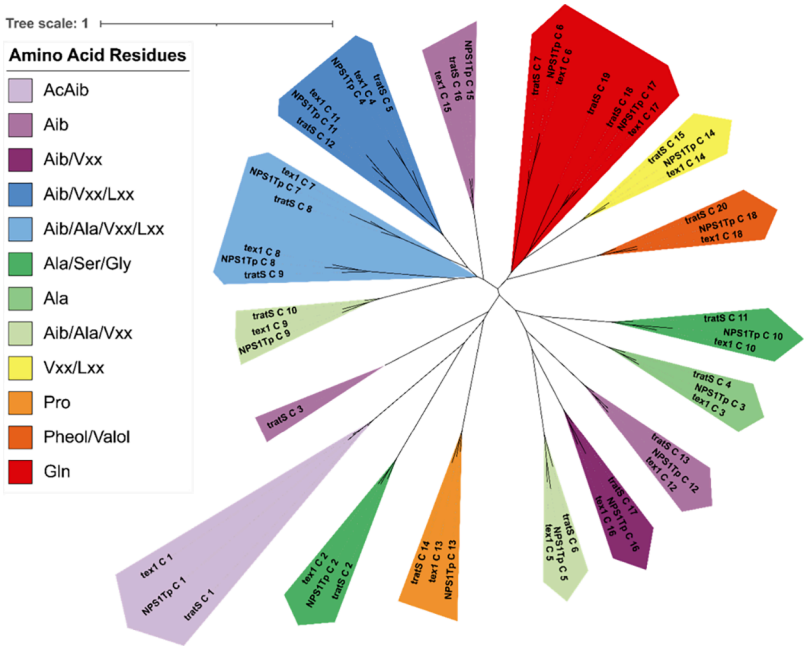

Figure 7. Phylogenetic analysis of the C domains from TratS, Tex1, and NPS1$_{Tp}$, color coded by substrate specificity. Vxx refers to valine or isovaline, and Lxx refers to leucine or isoleucine.

HRMS, MS/MS, ECD, and biosynthesis gene cluster analysis. Even for MS and NMR analyses together, only few examples are found in the literature.[54] Considering that more than 1000 peptaibols have been isolated to date, only very few of these peptides have had biosynthesis gene clusters investigated.[55−61] A common feature observed for peptaibols by both peptide hydrolysis and amino acid derivatization analysis as well as by genomic analyses is the rare occurrence of D-amino acid residues in these peptides. Our results align with the genomes of these peptaibols, contributing to understand the evolution of these fungal NRPS peptides, which appear to exert relevant ecological functions for fungi adaptation.[62]

CONCLUSIONS

In summary, the large peptaibols trichokonins VI (**1**) and VIII (**2**) have been fully characterized by analysis of NMR, HRMS/

https://doi.org/10.1021/acsomega.5c05271
ACS Omega 2025, 10, 48293−48307

Table 4. Assessment of *In Vitro* Antiplasmodial Activity (IC_{50}), Cytotoxicity (CC_{50}), and Selectivity Index Values of Trichokonins VI (1) and VIII (2), Trichogin A IV (3), and Hypocrin NPDG F (4)

compound	IC_{50}^{3D7} (μM) Mean ± SD	CC_{50}^{HepG2} (μM) Mean ± SD	SI[a]
trichokonins VI (1)	1.0 ± 0.2	28 ± 3	28
trichokonins VIII (2)	0.9 ± 0.2	15 ± 3	16
trichogin A IV (3)	5.7 ± 0.6	>25	>4
hypocrin NPDG F (4)	4.4 ± 0.9	>12	>3
artesunate[b]	15 ± 5 nM	nd	nd
pyrimethamine[b]	51 ± 9 nM	nd	nd

[a]SI = CC_{50}/IC_{50}. [b]Positive control for inhibition; nd = not determined.

MS, and ECD data for the first time. Analysis of *Trichoderma* sp. L2-2 enabled the assignment of the biosynthesis gene clusters of both peptaibols, which also displayed antiplasmodial activity against *P. falciparum* at the low micromolar range and attractive selectivity indexes.

EXPERIMENTAL SECTION

General Experimental Procedures. UV spectra were recorded on a Shimadzu UV-3600 instrument. Specific rotations were performed in a Polartronic H Schimidt +Haensch polarimeter with a 10 dm cuvette. CD spectra were obtained by using a Jasco J-815 spectropolarimeter. ATR-IR spectra were acquired with Shimadzu equipment, model IRAffinity. NMR spectra were obtained at 25 °C, in diluted aliquots in DMSO-d_6 or in MeOH-d_4, using TMS or the nondeuterated residual solvent signal as an internal standard, using a Bruker AVANCE III 14.1 T instrument operating at either 600 MHz (^{1}H) or 150 MHz (^{13}C), equipped with a cryo-probe TCI (^{1}H/^{13}C/^{15}N) of 5 mm with ATMA and field gradient in z. HRMS analyses were performed by Waters UPLC Xevo G2-XS q-TOF equipment using a C_{18} reverse phase column (Waters ACQUITY UPLC BEH, 2.1 mm × 100 mm, 1.7 μm). Elution was performed with a mobile phase composed of (A) H_2O + 0.1% formic acid and (B) MeCN + 0.1% formic acid. The gradient used was: 0−9.0 min linear gradient from 10 to 100% B, from 9.0−10.0 min 10% B was maintained for column reconditioning. The mass spectrometer was adjusted according to the following parameters: MSE continuous mode, an m/z detection range of 200−5000 Da, electrospray ionization mode ESI, an acquisition time of 0.2 s, and a collision energy ramp of 20−30 V. HPLC-PDA-ELSD-MS analyses were performed with a Waters Alliance 2695 instrument connected online with a Waters 2996 PDA detector, followed by a Micromass ZQ 2000 detector with an ESI interface. The mass spectrometer operation was adjusted using the following conditions: capillary voltage, 3.00 kV; source block temperature, 100 °C; desolvation temperature, 350 °C; voltage cone, 25 V; electrospray ionization (ESI), operating in positive and negative modes, detection in a 400−1400 Da range with total ion chromatogram (TIC). Desolvation and cone gas flows were adjusted to 50 and 350 L h^{-1}, respectively, with a N_2 source. Data recording and processing were performed using Empower 2.0 software. HPLC-PDA-ELSD-MS analyzes were acquired using a C_{18} reversed-phase column (Waters X-terra, 250 × 4.6 mm, 5 μm) with an eluent flow rate of 1 mL min^{-1}. Elution was performed with a mobile phase composed of (A) H_2O + 0.1% formic acid and (B) 1:1 (v/v) MeOH/MeCN + 0.1% formic acid. The gradient used was: 0−1.0 min with 10% B, linear gradient up to 100% B from 1.0−30.0 min, from 30.0−35.0 min 100% B was maintained and from 35.0 to 40.0 min, 10% B was maintained for column reconditioning, totaling 40 min of analysis. The sample volume injected was 20 μL of a solution with a concentration of 1.0−2.5 mg L^{-1}.

***Trichoderma* sp. L2-2 Identification.** The *Trichoderma* sp. L2-2 sample was isolated from a lichen substrate collected at King George Island (Admiralty Bay, Punta Plaza, Antarctica). The fungus was identified by analysis of the ITS genome sequence, which was deposited in GenBank with accession number MG813420.1. The fungal strain is stored in the Laboratory of Environmental and Industrial Mycology (LAMAI) collection associated with the Central of Microbial Resources of São Paulo State University CRM-UNESP (UNESP, Rio Claro, SP, Brazil). The fungus accession numbers are LAMAI 605 and CRM 55.

Extraction and Isolation. The *Trichoderma* sp. L2-2 strain was grown in 4 L of malt 2% medium at 15 °C with shaking (150 rpm). After 7 days of growth, the fungal cultures were filtered and blended with EtOAc. The organic solvent was separated from cultures by liquid−liquid partitioning. The EtOAc fraction was evaporated and solubilized in MeOH. The MeOH fraction was defatted with *n*-hexane. The resulting MeOH soluble fraction was named AT1M (0.77 g). The AT1M fraction was subjected to a solid-phase extraction (SPE) using prepacked silica gel columns derivatized with cyanopropyl groups. The following elution gradient was used: 100% Hex (AT1MA1), 100% CH_2Cl_2 (AT1MA2), CH_2Cl_2:EtOAc (1:1, v/v) (AT1MA3), 100% EtOAc (AT1MA4), EtOAc:MeOH (1:1, v/v) (AT1MA5), and 100% MeOH (AT1MA6). The fractions obtained (AT1MA1 to AT1MA6) were analyzed by HPLC-PDA-MS. Analysis of fraction AT1M5 by HPLC-PDA-MS indicated compounds with molecular weights higher than 500 Da.

Separation of the AT1M5 fraction (337.1 mg) was performed on a column packed with Sephadex LH-20 eluted with MeOH, collecting fractions of 4.5 mL. The fractions obtained were pooled by chromatographic similarity observed by TLC analysis [EtOAc/Hex (3:7, v/v), EtOAc/Hex (6:4, v/v), 100% EtOAc, MeOH/CH_2Cl_2 (1:9, v/v), MeOH/CH_2Cl_2 (3:7, v/v)]. A total of 14 fractions were obtained and named from AT1M5A to AT1M5P. Fraction AT1M5O (176.4 mg) was purified by semipreparative HPLC using a C_8 HPLC column (GL Sciences InertSustain, 250 × 4.6 mm, 5 μm) and an isocratic eluent of MeOH/H_2O (82:12, v/v) with 0.1% formic acid. The chromatographic separation was performed over 30 min (flow rate of 2.0 mL min^{-1} and detection by ELSD) yielding pure compounds TK-VI (**1**, 69.5 mg) and TK-VIII (**2**, 52.3 mg) (see the Supporting Information for details). The peptaibols TK-VI (**1**) and TK-VIII (**2**) were identified by NMR, HRMS, and IR analyses.

AT1M3 fraction (50.6 mg) was resubmitted to a solid-phase extraction using a prepacked column with a stationary phase of silica gel derivatized with diol groups. The sample was eluted with 10 mL of a gradient of EtOAc and Hex (from 20 to 100% of EtOAc), and 10 mL of a gradient of MeOH and EtOAc (from 20 to 100% MeOH) collecting fractions of 2.5 mL. The fractions obtained were grouped according to the polarity of the compounds observed in TLC analysis, resulting in 11 fractions named AT1M3A to AT1M3K. Fraction AT1M3I

https://doi.org/10.1021/acsomega.5c05271
ACS Omega 2025, 10, 48293−48307

(13.7 mg) was purified on an analytical column with a C_8 stationary phase column (GL Sciences InertSustain, 250 × 4.6 mm, 5 μm), isocratic eluent MeOH/H_2O (76:24, v/v) with 0.1% formic acid (flow rate of 1.0 mL min^{-1} and detection by ELSD). Four pure compounds were obtained: trichogin A IV (**3**, 5.1 mg), hypocrin NPDG F (**4**, 1.6 mg), hypocrin NPDG H (**5**, 1.8 mg), and trikoningin KB I (**6**, 0.4 mg). The peptaibols **3**−**5** were identified by NMR, HRMS, and IR analyses, and compound **6** was identified by HRMS/MS.

Marfey's Analysis. In a 2 mL glass vials, to a 1.0 mg of each amino acid standard were added 200 μL of H_2O, 80 μL of 1 M $NaHCO_3$ aqueous solution, and 400 μL of a solution of 1% Marfey's reagent (N_α-(2,4-dinitro-5-fluorophenyl)-L-alaninamide) in acetone. The reaction mixtures were stirred at 40 °C for 1 h. After this period, the reactions were quenched by the addition of 40 μL of a 2 N HCl aqueous solution. The resulting reaction mixture was dried, and the solid formed was dissolved in 2.0 mL of MeOH. After, 500 μL of these solutions were transferred to new vials and had their volumes completed to 1.0 mL with MeOH. These solutions were analyzed individually by HPLC-PDA-MS (as described in general procedures experiments). In addition, aliquots of all derivatized standards were combined to provide a mixed standard, which was: mixture 1: (L)-Leu and (L)-Ile; mixture 2: (L)-Val, (L)-Leu and (L)-Ile; mixture 3: (L)-Pro, (L)-Gln, (L)-Ala, (L)-Val and (L)-Leu. HPLC-PDA-MS analyses was performed using as mobile phase the gradient: 0−1.0 min with 20% B, linear gradient up to 100% B from 1.0−30.0 min, from 30.0−35.0 min maintained in 100% B, and finally from 35.0−40.0 min maintained in 10% B for column reconditioning.

To generate hydrolyzed and derivatized peptaibols, approximately 0.3−0.5 mg of compounds **1**−**5** were weighed separately into 2 mL vials. To these flasks was added 0.5 mL of an aqueous solution of HCl 6N. The reaction remained under stirring for 24 h, at 90 °C. Afterward, the solvent was evaporated, and to each compound, 100 μL of H2O, 40 μL of 1 M $NaHCO_3$ aqueous solution, and 200 μL of a solution of 1% Marfey's reagent in acetone were added. The reaction mixtures were stirred at 40 °C for 1 h. After this period, the reactions were quenched by the addition of 20 μL of 2 N HCl. The reaction mixtures were dried and dissolved in 1.0 mL of MeOH. Each hydrolyzed and derivatized compound was analyzed individually by HPLC-PDA-MS using the same mobile phase used for the analysis of the mixtures (chromatograms available at the Supporting Information).

Genome Sequencing and Mining. *Trichoderma* sp. L2-2 genomic DNA was purified by phenol-chloroform extraction. The UV−vis absorption spectrum of the DNA solution was obtained on a microvolume spectrophotometer (DeNovix DS-11), with 1 μL of solution added to the sample surface, using the preconfigured method for double-stranded DNA analysis. The DNA integrity was checked by electrophoresis analysis on 1% agarose gel. Genomic DNA was prepared for sequencing by employing an Illumina DNA Prep kit following the instructions of the manufacturer. Sequencing the library was performed on an Illumina NovaSeq6000 instrument, employing paired end, 2 × 150 base sequencing. Sequence data were processed for *de novo* assembly using the CLC genomics workbench (v22) using default parameters. DNA sequencing and assembly were performed by the University of Illinois at Chicago Core for Research Informatics (UICCRI).

Secondary metabolite biosynthesis gene clusters were preliminary identified using antiSMASH,[34] and the BGC related to the production of trichokonin VI and VIII was reannotated using the Augustus[43] platform with *Fusarium graminearum* as a reference. This BGC was named *trat* (GenBank accession no. PX023957). Coding sequences were investigated using NCBI's BLASTp.[44] Sequence data were visualized using Geneious Prime.

The synteny analysis of the *Trichoderma* sp. L2-2 and known peptaibols' BGCs was performed by Clinker using default parameters and visualized by the interactive clustermap.js.[47]

Maintenance of *P. falciparum In Vitro* Cultures. Continuous *in vitro* cultures of *P. falciparum* (3D7 strain) were maintained following a modified published method.[63] The procedure for this assay followed the protocol recently reported by us.[64]

SYBR Green I Growth Inhibition Assay against *P. falciparum* Asexual Forms. Compounds were diluted to a stock concentration of 20 mM in 100% DMSO prior to experiments and stored at −20 °C. Parasites were synchronized using sterile 5% (m/v) D-sorbitol treatment for 10 min at 37 °C to enrich ring-stage parasites.[65] All tests were conducted in duplicates using a SYBR Green I method with results compared to control cultures.[66] Concentration−response curves were generated, and half-maximal inhibitory concentration (IC_{50}^{3D7}) values for each compound were determined by nonlinear regression analysis (Figures S44−S46). Each IC_{50}^{3D7} value reflects the mean and standard deviations from at least two independent experiments. The detailed protocol used was recently described by us.[64]

Cultivation of Human Hepatocellular Carcinoma Cells (HepG2 Cell Line) and Cytotoxicity Evaluation. The cytotoxic effects of trichokonins **1**−**4** were evaluated against the human hepatocellular carcinoma cell line (HepG2). The assay procedure was conducted according to a previously published protocol.[64] Concentration−response curves were generated, and half-maximal inhibitory concentration (CC_{50}) values for each compound were calculated by using nonlinear regression analysis (Figures S44−S46). Each CC_{50} value is expressed as the mean ± standard deviation from at least two independent experiments. The selectivity index (SI) was determined by calculating the ratio of CC_{50} to IC_{50}^{3D7}.

■ ASSOCIATED CONTENT

Data Availability Statement

Raw NMR data have been provided within the NP-MRD platform. NP-MRD Deposit data for the compounds: trichokonin VI NP-Card ID: NP0351250; trichokonin VIII NP-Card ID: NP0351251; trichogin A IV NP-Card ID: NP0342304; hypocrin NPDG F NP-Card ID: NP0351252; hypocrin NPDG H NP-Card ID: NP0351253.

Supporting Information

The Supporting Information is available free of charge at https://pubs.acs.org/doi/10.1021/acsomega.5c05271.

NMR, HRMS, ECD, UV spectra of trichokonins VI and VIII; UPLC-HRMS analysis of Marfey AA derivatives; sequencing and biosynthesis gene cluster data of trichokonins VI and VIII; and concentration−response curves of trichokonins VI and VIII against *P. falciparum* (PDF)

https://doi.org/10.1021/acsomega.5c05271
ACS Omega 2025, 10, 48293−48307

AUTHOR INFORMATION

Corresponding Authors

Marcelo R. de Amorim − *Instituto de Química de São Carlos, Universidade de São Paulo, São Carlos, SP 13560-970, Brazil*; Email: marcamorim20@gmail.com

Sydney M. Schoellhorn − *Department of Chemistry and BioDiscovery Institute, University of North Texas, Denton, Texas 76203, United States*; orcid.org/0000-0001-8552-9402; Email: sydneyschoellhorn@my.unt.edu

Rafael Victorio Carvalho Guido − *São Carlos Institute of Physics, University of São Paulo, São Carlos, SP 13566-590, Brazil*; Email: rvcguido@usp.br

Roberto G. S. Berlinck − *Instituto de Química de São Carlos, Universidade de São Paulo, São Carlos, SP 13560-970, Brazil*; orcid.org/0000-0003-0118-2523; Email: rgsberlinck@iqsc.usp.br

Authors

Ariane F. Bertonha − *Instituto de Química de São Carlos, Universidade de São Paulo, São Carlos, SP 13560-970, Brazil; Brazilian Biosciences National Laboratory (LNBio), Brazilian Center for Research in Energy and Materials (CNPEM), Campinas, SP 13083-970, Brazil*; orcid.org/0000-0002-6651-8641

David E. Williams − *Departments of Chemistry and EOAS, University of British Columbia, Vancouver, BC V6T 1Z6, Canada*; orcid.org/0000-0001-5824-6415

Karen J. Nicacio − *Instituto de Química de São Carlos, Universidade de São Paulo, São Carlos, SP 13560-970, Brazil; Universidade Federal de Mato Grosso (UFMT), Cuiabá, MT 78060-900, Brazil*; orcid.org/0000-0001-9790-5786

Anna Caroline C. Aguiar − *Department of Microbiology, Immunology and Parasitology, Federal University of São Paulo, São Paulo, SP 04023-062, Brazil*; orcid.org/0000-0003-0139-8279

Talita Alvarenga Valdes − *São Carlos Institute of Physics, University of São Paulo, São Carlos, SP 13566-590, Brazil*

Giovana Rossi Mendes − *São Carlos Institute of Physics, University of São Paulo, São Carlos, SP 13566-590, Brazil*

Igor M. R. Moura − *São Carlos Institute of Physics, University of São Paulo, São Carlos, SP 13566-590, Brazil*; orcid.org/0000-0003-3279-6894

Lamonielli F. Michaliski − *Instituto de Química de São Carlos, Universidade de São Paulo, São Carlos, SP 13560-970, Brazil*

Matheus Gotha − *Instituto de Química de São Carlos, Universidade de São Paulo, São Carlos, SP 13560-970, Brazil*

Caue A. W. Zuccarino − *Instituto de Química de São Carlos, Universidade de São Paulo, São Carlos, SP 13560-970, Brazil*

Lara D. Sette − *Departamento de Biologia Geral e Aplicada, Universidade Estadual Paulista (UNESP), Instituto de Biociências, Rio Claro, SP 13506-900, Brazil*

Antônio G. Ferreira − *Departamento de Química, Universidade Federal de São Carlos, São Carlos, SP 13565-905, Brazil*

Raymond J. Andersen − *Departments of Chemistry and EOAS, University of British Columbia, Vancouver, BC V6T 1Z6, Canada*; orcid.org/0000-0002-7607-8213

Complete contact information is available at: https://pubs.acs.org/10.1021/acsomega.5c05271

Author Contributions

Ariane F. Bertonha: conceptualization, methodologies, visualization, formal analysis, investigation, writing, review, and editing. David E. Williams: formal analysis and editing draft. Karen J. Nicacio: formal analysis and investigation. Marcelo R. de Amorim: conceptualization, methodologies, visualization, formal analysis, investigation, writing, review, and editing. Sydney M. Schoellhorn: conceptualization, methodologies, visualization, formal analysis, investigation, writing, review, and editing. Anna Caroline C. Aguiar: methodologies, formal analysis, and investigation. Talita Alvarenga Valdes: methodologies, formal analysis, and investigation. Giovana Rossi Mendes: methodologies, formal analysis, and investigation. Igor M. R. Moura: methodologies, formal analysis, and investigation. Lamonielli F. Michaliski: methodologies, formal analysis, and investigation. Matheus Gotha: methodologies, formal analysis, and investigation. Caue A. W. Zuccarino: samples curation and data curation. Lara D. Sette: methodologies, formal analysis, and investigation. Antônio G. Ferreira: methodologies, formal analysis, and investigation. Raymond J. Andersen: review and editing. Rafael V. C. Guido: conceptualization, formal analysis, investigation, resources, supervision, writing, review, and editing. Roberto G. S. Berlinck: conceptualization, methodologies, visualization, formal analysis, investigation, resources, supervision, writing, review, and editing.

Funding

The Article Processing Charge for the publication of this research was funded by the Coordenacao de Aperfeicoamento de Pessoal de Nivel Superior (CAPES), Brazil (ROR identifier: 00x0ma614).

Notes

The authors declare no competing financial interest.

ACKNOWLEDGMENTS

The authors thank the financial support provided by the São Paulo State Research Foundation (FAPESP), Brazil, to R.V.C.G. (grants 2013/07600-3 and 2024/04805-8), to R.G.S.B. (grants 2015/01017-0 and 2019/17721-9), to A.C.C.A. (postdoctoral scholarship 2015/18192-9), to M.R.A. (postdoctoral scholarship 2020/01229-5), to T.A.V. (postdoctoral scholarship 2024/04949-0), to G.R.M. (PhD scholarship 2022/01063-5), to I.M.R.M. (PhD scholarship 2021/03977-1), to L.F.M. (PhD scholarship 2019/07894-3 and 2022/07831-4), to L.P.I. (PhD scholarships 2016/05133-7 and 2018/10742-8), and to M.G. (undergraduate research scholarship and PhD scholarship 2021/07343-7 and 2023/17676-9) and by the Brazilian National Council for Scientific and Technological Development (CNPq) to R.G.S.B. (senior research scholarship 304247/2021-9), to R.V.C.G. (senior research scholarship 310602/2021-1), to A.G.F. (senior research scholarship 304599/2022-0), and to the Coordenação de Aperfeiçoamento de Pessoal de Nível Superior-Brazil (CAPES) Finance Code 001. This project was also supported by the Agriculture and Food Research Initiative Competitive Grants Program Education and Workforce Development Program (project award no. 2023-67011-40393 to S.M.S.) from the U.S. Department of Agriculture's National Institute of Food and Agriculture.

https://doi.org/10.1021/acsomega.5c05271
ACS Omega 2025, 10, 48293−48307

REFERENCES

(1) Duarte, A. W. F.; Santos, J. A.; Vianna, M. V.; Vieira, J. M. F.; Mallagutti, V. H.; Inforsato, F. J.; Wentzel, L. C. P.; Lario, L. D.; Rodrigues, A.; Pagnocca, F. C.; Pessoa Junior, A.; Sette, L. D. Cold-adapted enzymes produced by fungi from terrestrial and marine Antarctic environments. *Crit. Rev. Biotechnol.* **2018**, *38* (4), 600−619.

(2) Varrella, S.; Barone, G.; Tangherlini, M.; Rastelli, E.; Dell'Anno, A.; Corinaldesi, C. Diversity, ecological role and biotechnological potential of Antarctic marine fungi. *J. Fungi* **2021**, *7* (5), 391.

(3) Núñez-Pons, L.; Shilling, A.; Verde, C.; Baker, B. J.; Giordano, D. Marine terpenoids from polar latitudes and their potential applications in biotechnology. *Mar. Drugs* **2020**, *18* (8), 401.

(4) Arrieche, D.; Cabrera-Pardo, J. R.; San-Martin, A.; Carrasco, H.; Taborga, L. Natural products from Chilean and Antarctic marine fungi and their biomedical relevance. *Mar. Drugs* **2023**, *21* (2), 98.

(5) Dou, K.; Lu, Z.; Wu, Q.; Ni, M.; Yu, C.; Wang, M.; Li, Y.; Wang, X.; Xie, H.; Chen, J.; Zhang, C.; Druzhinina, I. S. MIST: a multilocus identification system for *Trichoderma*. *Appl. Environ. Microbiol.* **2020**, *86* (18), No. e01532-20.

(6) Bissett, J.; Gams, W.; Jaklitsch, W.; Samuels, G. J. Accepted *Trichoderma* names in the year 2015. *IMA Fungus* **2015**, *6* (2), 263−295.

(7) Pedrero-Méndez, A.; Cesarini, M.; Mendoza-Salido, D.; Petrucci, A.; Sarrocco, S.; Monte, E.; Hermosa, R. Trichoderma strain-dependent direct and indirect biocontrol of Fusarium head blight caused by Fusarium graminearum in wheat. *Microbiol. Res.* **2025**, *296*, No. 128153.

(8) Yan, L.; Ali Khan, R. A. Biological control of bacterial wilt in tomato through the metabolites produced by the biocontrol fungus, *Trichoderma harzianum*. *Egypt. J. Biol. Pest Control* **2021**, *31*, 5.

(9) Mukhopadhyay, R.; Kumar, D. Trichoderma: a beneficial antifungal agent and insights into its mechanism of biocontrol potential. *Egypt. J. Biol. Pest Control* **2020**, *30*, 130.

(10) Guo, Q.; Shi, L.; Wang, X.; Li, D.; Yin, Z.; Zhang, J.; Ding, G.; Chen, L. Structures and biological activities of secondary metabolites from the Trichoderma genus (Covering 2018−2022). *J. Agric. Food Chem.* **2023**, *71* (37), 13612−13632.

(11) Abdenaceur, R.; Farida, B.-t; Mourad, D.; Rima, H.; Zahia, O.; Fatma, S.-H. Effective biofertilizer *Trichoderma* spp. isolates with enzymatic activity and metabolites enhancing plant growth. *Int. Microbiol* **2022**, *25* (4), 817−829.

(12) Luo, N.; Jiao, Y.; Ling, J.; Li, Z.; Zhang, W.; Zhao, J.; Li, Y.; Mao, Z.; Li, H.; Xie, B. Synergistic effect of two peptaibols from biocontrol fungus *Trichoderma longibrachiatum* strain 40418 on CO-induced plant resistance. *J. Agric. Food Chem.* **2024**, *72* (38), 20763−20774.

(13) Yin, Y.; Zhu, G.; Wu, J.; She, Z.; Yuan, J.; Wang, B. Isolation of two peptaibols with potent antimicrobial and cytotoxic activities from the mangrove endophytic fungus *Trichoderma lentiforme* ML-P8−2. *Nat. Prod. Res.* **2024**, *39*, 3376−3381.

(14) Castro, G. S.; Sousa, T. F.; da Silva, G. F.; Pedroso, R. C. N.; Menezes, K. S.; Soares, M. A.; Dias, G. M.; Santos, A. O.; Yamagishi, M. E. B.; Faria, J. V.; Januário, A. H.; Koolen, H. H. F. Characterization of peptaibols produced by a marine strain of the fungus *Trichoderma endophyticum* via mass spectrometry, genome mining and phylogeny-based prediction. *Metabolites* **2023**, *13*, 221.

(15) Valiyambath, V. K.; Thomas, T. A.; George, P.; Neettiyath Kalathil, L.; Kaprakkaden, A.; Subraya, K. K.; Raghavan, D.; Ravindran, P. Characterization and quantification of peptaibol produced by novel *Trichoderma* spp: harnessing their potential to mitigate moisture stress through enhanced biochemical and physiological responses in black pepper (*Piper nigrum* L.). *World J. Microbiol. Biotechnol.* **2024**, *40*, 330.

(16) Alfaro-Vargas, P.; Bastos-Salas, A.; Muñoz-Arrieta, R.; Pereira-Reyes, R.; Redondo-Solano, M.; Fernández, J.; Mora-Villalobos, A.; López-Gómez, J. P. Peptaibol production and characterization from *Trichoderma asperellum* and their action as biofungicide. *J. Fungi* **2022**, *8*, 1037.

(17) Daniel, J. F. S.; Rodrigues Filho, E. Peptaibols of Trichoderma. *Nat. Prod. Rep.* **2007**, *24* (5), 1128−1141.

(18) de Amorim, M. R.; Barbosa, C. d. S.; Paz, T. A.; Ióca, L. P.; Nicácio, K. J.; de Oliveira, L. F. P.; Goulart, M. O.; Paulino, J. M.; da Cruz, M. O.; Ferreira, A. G.; Furlan, M.; de Lira, S. P.; dos Santos, R. A.; Rodrigues, A.; Guido, R. V. C.; Berlinck, R. G. S. Polyketide- and terpenoid-derived metabolites produced by a marine-derived fungus Peroneutypa sp. *J. Nat. Prod.* **2023**, *86*, 1476−1486.

(19) de Amorim, M. R.; Schoellhorn, S. M.; Barbosa, C. D. S.; Mendes, G. R.; Macedo, K. d. L.; Ferreira, A. G.; Venâncio, T.; Guido, R. V. C.; Batista, A. N. L.; Batista, J. M.; Skellam, E.; Berlinck, R. G. S. Structure and biosynthesis of perochalasins a-c, open-chain merocytochalasans produced by the marine-derived fungus *Peroneutypa* sp. M16. *J. Nat. Prod.* **2024**, *87* (9), 2204−2215.

(20) da Silva Oliveira, L.; Crnkovic, C. M.; de Amorim, M. R.; Navarro-Vázquez, A.; Paz, T. A.; Freire, V. F.; Takaki, M.; Venâncio, T.; Ferreira, A. G.; de Freitas Saito, R.; Chammas, R.; Berlinck, R. G. S. Phomactinine, the first nitrogen-bearing phomactin, produced by *Biatriospora* sp. CBMAI 1333. *J. Nat. Prod.* **2023**, *86* (8), 2065−2072.

(21) Gotha, M.; Junqueira, G. C.; Bertonha, A. F.; Rodríguez, J. P. G.; Gubiani, J. R.; Pissinati, E. F.; Lima, R. N.; Sette, L. D.; de Lira, S. P.; Oliveira, L. F. P.; Batista, A. N. L.; Batista, J. M.; Ferreira, A. G.; Paixão, M. W.; Amorim, M. R.; Berlinck, R. G. S. Water-soluble amino acid derivatives isolated from cultures of three fungal strains. *Phytochem. Lett.* **2024**, *64*, 123−132.

(22) Santucci, P. M.; de Oliveira, C. R.; Monteiro, A. F.; Mendes, G. R.; de Amorim, M. R.; Rosa, G. H. S.; Sette, L. D.; Marchi, R. C.; Deflon, V. M.; dos Santos, P. H. T.; Carvalho, G. G.; Brocchi, M.; Guido, R. V. C.; Ferreira, A. G.; de Oliveira, K. T.; Berlinck, R. G. S. Improved production of palitantin by design of experiments and semi-synthesis of palitantin derivatives for bioactivity assessment. *Fitoterapia* **2025**, *180*, No. 106310.

(23) Huang, Q.; Tezuka, Y.; Kikuchi, T.; Nishi, A.; Tubaki, K.; Tanaka, K. Studies on metabolites of mycoparasitic fungi. II. Metabolites of *Trichoderma koningii*. *Chem. Pharm. Bull.* **1995**, *43* (2), 223−229.

(24) Huang, Q.; Tezuka, Y.; Kikuchi, T.; Momose, Y. Trichokonin-VI, a New Ca^{2+} Channel Agonist in Bullfrog Cardiac Myocytes. *Eur. J. Pharmacol.* **1994**, *271*, R5−R6.

(25) Song, X. Y.; Xie, S. T.; Chen, X. L.; Sun, C. Y.; Shi, M.; Zhang, Y. Z. Solid-state fermentation for Trichokonins production from *Trichoderma koningii* SMF2 and preparative purification of Trichokonin VI by a simple protocol. *J. Biotechnol.* **2007**, *131*, 209−205.

(26) (a) Shi, M.; Wang, H. N.; Xie, S. T.; Luo, Y.; Sun, C. Y.; Chen, X. L.; Zhang, Y. Z. Antimicrobial peptaibols, novel suppressors of tumor cells, targeted calcium-mediated apoptosis and autophagy in human hepatocellular carcinoma cells. *Molecular Cancer* **2010**, *9*, 26. (b) Shi, M.; Zhang, T.; Sun, L.; Luo, Y.; Liu, D.-H.; Xie, S.-T.; Song, X.-Y.; Wang, G.-F.; Chen, X.-L.; Zhou, B.-C.; Zhang, Y.-Z. Calpain, Atg5 and Bak play important roles in the crosstalk between apoptosis and autophagy induced by influx of extracellular calcium. *Apoptosis* **2013**, *18*, 435−451.

(27) Shi, M.; Chen, L.; Wang, X. W.; Zhang, T.; Zhao, P. B.; Song, X. Y.; Sun, C. Y.; Chen, X. L.; Zhou, B. C.; Zhang, Y. Z. Antimicrobial peptaibols from *Trichoderma pseudokoningii* induce programmed cell death in plant fungal pathogens. *Microbiology-SGM* **2012**, *158*, 166−175.

(28) Shi, W. L.; Chen, X. L.; Wang, L. X.; Gong, Z. T.; Li, S. Y.; Li, C. L.; Xie, B. B.; Zhang, W.; Shi, M.; Li, C. Y.; Zhang, Y. Z.; Song, X. Y. Cellular and molecular insight into the inhibition of primary root growth of *Arabidopsis* induced by peptaibols, a class of linear peptide antibiotics mainly produced by *Trichoderma* spp. *J. Exp. Bot.* **2016**, *67*, 2191−2205.

(29) Zhao, P. B.; Ren, A. Z.; Dong, P.; Sheng, Y. S.; Chang, X.; Zhang, X. S. The antimicrobial peptaibol trichokonin IV promotes plant growth and induces systemic resistance against *Botrytis cinerea* infection in moth orchid. *J. Phytopathol.* **2018**, *166*, 346−354.

(30) Goulart, M. O.; Paulino, J. M.; Silveira, N. N.; Bertonha, A. F.; Berlinck, R. G. S.; Santos, R. A. Isolation and comparative

https://doi.org/10.1021/acsomega.5c05271
ACS Omega 2025, 10, 48293−48307

genotoxicity screening of trichokonins VI and VIII on CHO-K1 cells. *Drug Chem. Toxicol.* **2025**, *48*, 521−529.
(31) Winter, H. L.; Flores-Bocanegra, L.; Cank, K. B.; Crandall, W. J.; Rotich, F. C.; Tillman, M. N.; Todd, D. A.; Graf, T. N.; Raja, H. A.; Pearce, C. J.; Oberlies, N. H.; Cech, N. B. What was old is new again: Phenotypic screening of a unique fungal library yields pyridoxatin, a promising lead against extensively resistant *Acinetobacter baumannii* (AB5075). *Phytochem. Lett.* **2023**, *55*, 88−96.
(32) Auvin-Guette, C.; Rebuffat, S.; Bodo, B.; Prigent, Y. Trichogin A IV, an 11-residue lipopeptaibol from *Trichoderma longibrachiatum*. *J. Am. Chem. Soc.* **1992**, *114* (6), 2170−2174.
(33) Zotti, M. D.; Biondi, B.; Peggion, C.; Formaggio, F.; Park, Y.; Hahm, K. S.; Toniolo, C. Trichogin GA IV: a versatile template for the synthesis of novel peptaibiotics. *Org. Biomol. Chem.* **2012**, *10* (6), 1285−1299.
(34) Lee, J. W.; Collins, J. E.; Wendt, K. L.; Chakrabarti, D.; Cichewicz, R. H. Leveraging peptaibol biosynthetic promiscuity for next-generation antiplasmodial therapeutics. *J. Nat. Prod.* **2021**, *84* (2), 503−517.
(35) Auvin-Guette, C.; Rebuffat, S.; Vuidepot, I.; Massias, M.; Bod, B. Structural elucidation of trikoningins KA and KB, peptaibols from *Trichoderma koningii*. *J. Chem. Soc., Perkin Trans. 1* **1993**, *1*, 249−255.
(36) Peggion, C.; Piazza, C.; Formaggio, F.; Crisma, M.; Toniolo, C.; Kaptein, B.; Broxterman, Q. B.; Kamphuis, J. Synthesis, conformation, and membrane modifying properties of the trikoningin KB lipopeptaibols: effect of hydrophobicity and chirality in position 1. *Lett. Pept. Sci.* **2000**, *7*, 9−16.
(37) Marik, T.; Tyagi, C.; Balázs, D.; Urbán, P.; Szepesi, Á.; Bakacsy, L.; Endre, G.; Rakk, D.; Szekeres, A.; Andersson, M. A.; Salonen, H.; Druzhinina, I. S.; Vágvölgyi, C.; Kredics, L. Structural diversity and bioactivities of peptaibol compounds from the *Longibrachiatum* clade of the filamentous fungal genus *Trichoderma*. *Front. Microbiol.* **2019**, *10*, 1434.
(38) Marik, T.; Várszegi, C.; Kredics, L.; Vágvölgyi, C.; Szekeres, A. Mass spectrometric investigation of alamethicin. *Acta Biol. Szeged.* **2013**, *57* (2), 109−112.
(39) Suwan, S.; Isobe, M.; Kanokmedhakul, S.; Lourit, N.; Kanokmedhakul, K.; Soytong, K.; Koga, K. Elucidation of high micro-heterogeneity of an acidic-neutral trichotoxin mixture from *Trichoderma harzianum* by electrospray ionization quadrupole time-of-flight mass spectrometry. *J. Mass Spectrom.* **2000**, *35*, 1438−1451.
(40) Rivera-Chávez, J.; Raja, H. A.; Graf, T. N.; Burdette, J. E.; Pearce, C. J.; Oberlies, N. H. Biosynthesis of fluorinated peptaibols using a site-directed building block incorporation approach. *J. Nat. Prod.* **2017**, *80* (6), 1883−1892.
(41) Whitmore, L.; Wallace, B. A. Peptaibols. In *Handbook of Biologically Active Peptides*, Kastin, A. J. Ed.; Academic Press, 2006; pp 83−88.
(42) Blin, K.; Shaw, S.; Kloosterman, A. M.; Charlop-Powers, Z.; Van Wezel, G. P.; Medema, M. H.; Weber, T. AntiSMASH 6.0: improving cluster detection and comparison capabilities. *Nucleic Acids Res.* **2021**, *49* (W1), W29−W35.
(43) Keller, O.; Kollmar, M.; Stanke, M.; Waack, S. A novel hybrid gene prediction method employing protein multiple sequence alignments. *Bioinformatics* **2011**, *27* (6), 757−763.
(44) Sayers, E. W.; Bolton, E. E.; Brister, J. R.; Canese, K.; Chan, J.; Comeau, D. C.; Connor, R.; Funk, K.; Kelly, C.; Kim, S.; Madej, T.; Marchler-Bauer, A.; Lanczycki, C.; Lathrop, S.; Lu, Z.; Thibaud-Nissen, F.; Murphy, T.; Phan, L.; Skripchenko, Y.; Tse, T.; Wang, J.; Williams, R.; Trawick, B. W.; Pruitt, K. D.; Sherry, S. T. Database resources of the national center for biotechnology information. *Nucleic Acids Res.* **2022**, *50* (D1), D20−D26.
(45) Wiest, A.; Grzegorski, D.; Xu, B. W.; Goulard, C.; Rebuffat, S.; Ebbole, D. J.; Bodo, B.; Kenerley, C. Identification of peptaibols from *Trichoderma virens* and cloning of a peptaibol synthetase. *J. Biol. Chem.* **2002**, *277* (23), 20862−20868.
(46) Viterbo, A.; Wiest, A.; Brotman, Y.; Chet, I.; Kenerley, C. The 18mer peptaibols from *Trichoderma virens* elicit plant defence responses. *Mol. Plant Pathol.* **2007**, *8* (6), 737−746.
(47) Gilchrist, C. L. M.; Chooi, Y.-H. Clinker & Clustermap.js: automatic generation of gene cluster comparison figures. *Bioinformatics* **2021**, *37* (16), 2473−2475.
(48) Marik, T.; Urbán, P.; Tyagi, C.; Szekeres, A.; Leitgeb, B.; Vágvölgyi, M.; Manczinger, L.; Druzhinina, I. S.; Vágvölgyi, C.; Kredics, L. Diversity profile and dynamics of peptaibols produced by green mould *Trichoderma* species in interactions with their hosts *Agaricus bisporus* and *Pleurotus ostreatus*. *Chem. Biodiversity* **2017**, *14*, No. e1700033.
(49) Collins, J. E.; Lee, J. W.; Rocamora, F.; Saggu, G. S.; Wendt, K. L.; Pasaje, C. F. A.; Smick, S.; Santos, N. M.; Paes, R.; Jiang, T.; Mittal, N.; Luth, M. R.; Chin, T.; Chang, H.; McLellan, J. L.; Morales-Hernandez, B.; Hanson, K. K.; Niles, J. C.; Desai, S. A.; Winzeler, E. A.; Cichewicz, R. H.; Chakrabarti, D. Antiplasmodial peptaibols act through membrane directed mechanisms. *Cell Chem. Biol.* **2024**, *31*, 312−325.
(50) Katsuno, K.; Burrows, J. N.; Duncan, K.; van Huijsduijnen, R. H.; Kaneko, T.; Kita, K.; Mowbray, C. E.; Schmatz, D.; Warner, P.; Slingsby, B. T. Hit and lead criteria in drug discovery for infectious diseases of the developing world. *Nat. Rev. Drug Discovery* **2015**, *14*, 751−758.
(51) Niu, X.; Thaochan, N.; Hu, Q. Diversity of Linear Non-Ribosomal Peptide in Biocontrol Fungi. *J. Fungi* **2020**, *6*, No. 61.
(52) Hou, X.; Sun, R.; Feng, Y.; Zhang, R.; Zhu, T.; Che, Q.; Zhang, Q.; Li, D. Peptaibols: Diversity, bioactivity, and biosynthesis. *Engin. Microbiol.* **2022**, *2*, No. 100026.
(53) Röhrich, C. R.; Iversen, A.; Jaklitsch, W. M.; Voglmayr, H.; Vilcinskas, A.; Nielsen, K. F.; Thrane, U.; von Döhren, H.; Brückner, H.; Degenkolb, T. Screening the Biosphere: The Fungicolous Fungus *Trichoderma phellinicola*, a Prolific Source of Hypophellins, New 17-, 18-, 19-, and 20-Residue Peptaibiotics. *Chem. Biodiv.* **2013**, *10*, 787−812.
(54) (a) Condamine, E.; Rebuffat, S.; Prigent, Y.; Ségalas, I.; Bodo, B.; Davoust, D. Three-dimensional structure of the ion-channel forming peptide trichorzianin TA VII bound to sodium dodecyl sulfate micelles. *Biopolymers* **1998**, *46*, 75−88. (b) Rebuffat, S.; Pringent, Y.; Auvin-Guette, C.; Bodo, B. Tricholongins BI and BII, 19-residue peptaibols from Trichoderma longibrachiatum. *Eur. J. Biochem.* **1991**, *46*, 661−674. (c) Anders, R.; Wenschuh, H.; Soskic, V.; Fischer-Frühholz, S.; Ohlenschläger, O.; Dornberger, K.; Brown, L. R. *J. Pept. Res.* **1998**, *52*, 34−44. (d) Kumazawa, S.; Kanda, M.; Aoyama, H.; Utagawa, M.; Ohtani, H.; Chiga, I.; Mikawa, T.; Hayase, T.; Hino, T. Nuclear Magnetic Resonance Study and Secondary Structure Determination of the Antibiotic Peptide. *Aibellin. Biosci. Biotechnol. Biochem.* **1994**, *58*, 2188−2192. (e) Auvin-Guette, C.; Rebuffat, S.; Vuidepot, I.; Massias, M.; Bodo, B. *J. Chem. Soc., Perkin Trans.* **1993**, *1*, 249−255. (f) Rebuffat, S.; Conraux, L.; Massias, M.; Auvinguette, C.; Bodo, B. Sequence and Solution Conformation of the 20-residue peptaibols, saturnisporins SA-II and SA-IV. *Int. J. Pept. Prot. Res.* **1993**, *41*, 74−84.
(55) Xiao, D.; Zhang, M.; Wu, P.; Li, T.; Li, W.; Zhang, L.; Yue, Q.; Chen, X.; Wei, X.; Xu, Y.; Wang, C. Halovirs I-K, antibacterial and cytotoxic lipopeptaibols from the plant pathogenic fungus Paramyrothecium roridum NRRL 2183. *J. Antibiot.* **2022**, *75*, 247−257.
(56) Sinichich, A. A.; Krivonos, D. V.; Baranova, A. A.; Zhitlov, M. Y.; Belozerova, O. A.; Lushpa, V. A.; Vvedensky, A. V.; Serebryakova, M. V.; Kalganova, A. I.; Kudzhaev, A. M.; Prokopenko, Y. A.; Sinelnikova, S. S.; Trusova, E. A.; Kovalchuk, S. I.; Ilina, E. N.; Terekhov, S. S.; Alferova, V. A. Genome-Guided Metabolomic Profiling of Peptaibol-Producing *Trichoderma*. *Int. J. Mol. Sci.* **2025**, *26*, No. 5599.
(57) Reiber, K.; Neuhof, T.; Ozegowski, J. H.; Von Döhren, H.; Schwecke, T. A nonribosomal peptide synthetase involved in the biosynthesis of ampullosporins in *Sepedonium ampullosporum*. *J. Pept. Sci.* **2003**, *9*, 701−713.
(58) Tehan, R. M.; Blount, R. R.; Goold, R. L.; Mattos, D. R.; Spatafora, N. R.; Tabima, J. F.; Gazis, R.; Wang, G.; Ishmael, J. E.; Spatafora, J. W.; McPhail, K. L. Tolypocladamide H and the Proposed

https://doi.org/10.1021/acsomega.5c05271
ACS Omega 2025, 10, 48293−48307

Tolypocladamide NRPS in *Tolypocladium* Species. *J. Nat. Prod.* **2022**, *85*, 1363−1373.
(59) Song, K. N.; Ai, Y. T.; Zhou, J. S.; Dun, B. Q.; Yue, Q.; Zhang, L. W.; Xu, Y. Q.; Wang, C. Isolation, Characterization, and Bioherbicidal Potential of the 16-Residue Peptaibols from *Emericellopsis* sp. XJ1056. *J. Agric. Food Chem.* **2024**, *72*, 6315−6326.
(60) Liang, X.; Yang, J.-F.; Huang, Z.-H.; Ma, X.; Yan, Y.; Qi, S.-H. New Antibacterial Peptaibiotics against Plant and Fish Pathogens from the Deep-Sea-Derived Fungus *Simplicillium obclavatum* EIODSF 020. *J. Agric. Food Chem.* **2024**, *72*, 6402−6413.
(61) Jiao, Y.; Ling, J.; Khan, R. A. A.; Luo, N.; Li, Z.; Li, Z.; Yang, Y.; Zhao, J.; Mao, Z.; Bills, G. F.; Xie, B.; Li, B. Genome Mining Reveals Biosynthesis of the Antifungal Lipopeptaibols, Texenomycins, through a Hybrid PKS-NRPS System, in the Fungus *Mariannaea elegans*. *J. Agric. Food Chem.* **2025**, *73*, 226−236.
(62) (a) Röhrich, C. R.; Jaklitsch, W. M.; Voglmayr, H.; Iversen, A.; Vilcinskas, A.; Nielsen, K. F.; Thrane, U.; von Döhren, H.; Brückner, H.; Degenkolb, T. Front line defenders of the ecological niche! Screening the structural diversity of peptaibiotics from saprotrophic and fungicolous *Trichoderma*/*Hypocrea* species. *Fungal Diversity* **2014**, *69*, 117−146. (b) Song, M.; Zhou, Y.; Li, G.; Barashkova, A. S.; Rogozhin, E. A.; Chang, W. Peptides in plant−microbe interactions: Functional diversity and pharmacological applications. *Cell Surface* **2025**, *13*, No. 100145. (c) Krain, A.; Siupka, P. Fungal Guttation, a Source of Bioactive Compounds, and Its Ecological Role—A Review. *Biomol.* **2021**, *11*, 1270.
(63) Trager, W.; Jenson, J. B. Cultivation of malarial parasites. *Nature* **1978**, *273*, 621−622.
(64) Mendes, G. R.; Noronha, A. L.; Moura, I. M. R.; Moreira, N. M.; Bonatto, V.; Barbosa, C. S.; Maluf, S. E. C.; Souza, G. E.; de Amorim, M. R.; Aguiar, A. C. C.; Cruz, F. C.; Ferreira, A. D. S.; Teles, C. B. G.; Pereira, D. B.; Hajdu, E.; Ferreira, A. G.; Berlinck, R. G. S.; Guido, R. V. C. Marine Guanidine Alkaloids Inhibit Malaria Parasites Development in In Vitro, In Vivo and Ex Vivo Assays. *ACS Inf. Dis.* **2025**, *11*, 1854−1867.
(65) Lambros, C.; Vanderberg, J. P. Synchronization of *Plasmodium falciparum* erythrocytic stages in culture. *J. Parasitol.* **1979**, *65*, 418−420.
(66) Vossen, M. G.; Pferschy, S.; Chiba, P.; Noedl, H. The SYBR green i malaria drug sensitivity assay: performance in low parasitemia samples. *Am. J. Trop. Med. Hyg.* **2010**, *82* (3), 398−401.

https://doi.org/10.1021/acsomega.5c05271
ACS Omega 2025, 10, 48293−48307